

DOI: 10.1070/QEL16219

In theory there is no difference between theory and practice; in practice there is.
Yogi Berra

Design of high-bit-rate coherent communication links

V.A. Konyshev, A.V. Leonov, O.E. Nanii, A.G. Novikov, V.N. Treshchikov, R.R. Ubaydullaev

Abstract. **We report an analysis of the problems encountered in the design of modern high-bit-rate coherent communication links. A phenomenological communication link model is described, which is suitable for solving applied tasks of the network design with nonlinear effects taken into account. We propose an engineering approach to the design that is based on the use of fundamental nonlinearity coefficients calculated in advance for the experimental configurations of communication links. An experimental method is presented for calculating the nonlinearity coefficient of communication links. It is shown that the proposed approach allows one to successfully meet the challenges in designing communication networks.**

Keywords: *optical communication, wavelength division multiplexing, coherent detection.*

1. Introduction

High-bit-rate coherent communication systems are being rapidly developed. Hardly had 40-Gbit s^{-1} communication systems [1] replaced the communication systems with a data rate of 10 Gbit s^{-1} when coherent communication systems with a bit rate of 100 Gbit s^{-1} per channel started to be mass-introduced throughout the world in 2013–2014 [2–4]. In 2015, there appeared commercial systems with a single-channel rate of 200 Gbit s^{-1} in the 2×200 Gbit s^{-1} format (400 Gbit s^{-1} per two channels) [5]. At OFC 2016 and ECOC 2016 conferences the leading producers announced that commercial systems with a channel bit rate of 400 Gbit s^{-1} are expected to be released in the early 2017. Accordingly, the methods of designing communication systems with dense wavelength-division multiplexing (DWDM systems) are being actively developed.

V.A. Konyshev T8 LLC, office 826, Krasnobogatyrskaya ul. 44/1, 107076 Moscow, Russia; Vavilov Institute of the History of Natural Science and Technology, Russian Academy of Sciences, Staropanskii per. 1/5, 109012 Moscow, Russia;
A.V. Leonov, A.G. Novikov, R.R. Ubaydullaev T8 LLC, office 826, Krasnobogatyrskaya ul. 44/1, 107076 Moscow, Russia; e-mail: leonov.av@t8.ru;
O.E. Nanii T8 LLC, office 826, Krasnobogatyrskaya ul. 44/1, 107076 Moscow, Russia; Faculty of Physics, M.V. Lomonosov Moscow State University, Vorob'evy gory, 119991 Moscow, Russia;
V.N. Treshchikov T8 LLC, office 826, Krasnobogatyrskaya ul. 44/1, 107076 Moscow, Russia; V.A. Kotel'nikov Institute of Radio Engineering and Electronics (Fryazino Branch), Russian Academy of Sciences, pl. Vvedenskogo 1, 141190 Fryazino, Moscow region, Russia

Received 30 September 2016; revision received 21 October 2016
Kvantovaya Elektronika **46** (12) 1121–1128 (2016)
Translated by I.A. Ulitkin

An important feature of high-bit-rate coherent systems with digital signal processing is the ability to digitally compensate for the dispersion in the processing of the signal in the receiver [6]. This makes it possible to transmit a high-bit-rate signal in the communication link without dispersion compensators. The accumulation of nonlinear signal distortions in the uncompensated lines does not follow the scenario of the dispersion-compensated lines. On the one hand, with a large dispersion at the span input*, nonlinear distortions in a single span of the communication line are higher. On the other hand, the correlation between nonlinear distortions in different spans is less than in spans of dispersion-compensated links [7–9]. Therefore, these approaches to the design, developed for dispersion-managed communication systems [10–13], do not apply to coherent communication systems without chromatic dispersion compensation in the link.

Calculation of nonlinear distortions is the most difficult task in the design of high-bit-rate coherent communication lines. Nonlinear distortions depend on many characteristics of the link: span lengths, attenuation in the fibre, power and dispersion at the input of each span, number and type of channels, frequency plan and guard interval, etc. The numerical simulation based on the solution of the nonlinear Schrödinger equation is a powerful tool for the analysis of physical phenomena in fibre-optic communication lines [14, 15], but it is difficult to apply to design problems due to the complexity and duration of the calculations and the need for large computational resources. There are theoretical formulae for calculating nonlinear distortions based on the characteristics of the optical fibre and the communication parameters of the system [16]; however, they are derived with a number of conditions taken into account [in particular, a large number of spans, a large number of channels, Nyquist wavelength division multiplexing (NyquistWDM), etc.]. These conditions are often not met in real communication systems, which makes these formulae unsuitable for computations and design of real communication lines.

From a practical point of view, the design of coherent optical communication lines requires an engineering calculation method that takes into account linear and nonlinear distortions and is based on the use of relatively simple empirical equations which allow for calculations of various configurations of the lines with a sufficiently small error. The development of such techniques is a complex scientific and technical and experimental problem. Approaches to solving this problem and the results obtained are presented in this paper.

* The dispersion at the input to the Nth span (accumulated dispersion) is used in reference to the total dispersion in an optical path from its beginning to the input to the Nth span.

2. Phenomenological communication link model

The most popular theoretical model to describe nonlinear distortions in coherent systems without dispersion compensation is the GN-model (Gaussian-noise model), which well describes the experimental results for long-haul communication links (more than five spans). Within the framework of this model, nonlinear distortions are treated as a Gaussian noise, additive to amplified spontaneous emission (ASE) noise [17–20]. The main provisions of the nonlinear noise model are confirmed experimentally and numerically [21–26]. It is assumed in this case that the bit error rate (BER) in the signal depends only on the total noise [sum of linear (ASE) and nonlinear (NL) noises] and is independent of the contribution of each type of noise in the total noise. This assumption allows us to construct a simple phenomenological model of communication lines, convenient for practical applications.

Hereafter, absolute values of the quantities are written in capital letters, and the corresponding logarithmic values are expressed in lower-case letters: $p = 10\lg P$. The total noise affecting the link is described in the GN-model by the expression

$$P_\Sigma = P_{\mathrm{ASE}} + P_{\mathrm{NL}}. \tag{1}$$

Dividing both sides of (1) by the signal power at the beginning of the span, P, we obtain

$$\frac{1}{\mathrm{OSNR}_{\mathrm{BER}}} = \frac{1}{\mathrm{OSNR}_{\mathrm{L}}} + \frac{1}{\mathrm{OSNR}_{\mathrm{NL}}}. \tag{2}$$

All the values of power in formula (2) must be given for the beginning of the span. The quantity $\mathrm{OSNR}_{\mathrm{BER}} = P/P_\Sigma$ is the ratio of the signal power to the total noise power, determining the bit error rate in the link. The relation between $\mathrm{OSNR}_{\mathrm{BER}}$ and BER in the model under study is one-to-one and described by the calibration curve of the transponder. The calibration curve is measured experimentally in the back-to-back (BTB) configuration* (with $P_{\mathrm{NL}} = 0$ and $P_\Sigma = P_{\mathrm{ASE}}$). An example of the calibration curve is shown in Fig. 1. The upper left point on this curve corresponds to a maximum value of bit errors in the signal (prior to application of forward error correction, FEC), at which the transponder is still able to receive the signal. In the example under study, it is equal to $\sim 1.92 \times 10^{-2}$. To this maximum permissible BER value there corresponds the threshold $\mathrm{OSNR}_{\mathrm{BER}}$, which is called 'the required OSNR of the transponder' and is referred to as $\mathrm{OSNR}_{\mathrm{BTB}}$ (sometimes the designations $\mathrm{OSNR}_{\mathrm{T}}$ and $\mathrm{OSNR}_{\mathrm{R\,BTB}}$ are used). This is one of the main technical characteristics of a transponder, which is always specified in the specification.

As a rule, for 10, 40 and 100-Gbit s^{-1} links, when the signal-to-noise ratio reaches an $\mathrm{OSNR}_{\mathrm{BTB}}$ value, the number of errors increases so dramatically that synchronisation is immediately lost. This behaviour is a consequence of the efficient operation of FEC algorithms. While $\mathrm{OSNR}_{\mathrm{BER}}$ at the transponder input is greater than $\mathrm{OSNR}_{\mathrm{BTB}}$, FEC algorithms successfully correct errors and the bit error rate after error correction does not exceed 10^{-12}. When $\mathrm{OSNR}_{\mathrm{BER}}$ at the transponder input becomes smaller than $\mathrm{OSNR}_{\mathrm{BTB}}$, FEC algorithms can no longer cope with the error correction in the received signal, which immediately leads to a sharp increase in bit errors on the client side and to the loss of synchronisation.

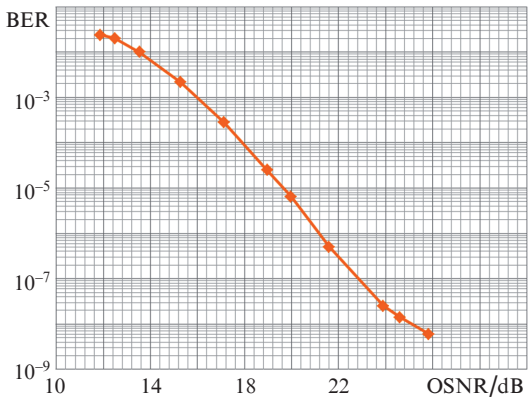

Figure 1. Example of a calibration curve of the transponder (100 Gbit s^{-1}).

The parameter $\mathrm{OSNR}_{\mathrm{L}} = P/P_{\mathrm{ASE}}$ is the ratio of the signal power to the ASE noise power. The value of the amplifier noise (at the end of the span) is defined by the formula $h\nu B \times (GF - 1) \approx h\nu BGF$, where B is the normalised bandwidth, G is the amplifier gain, and F is the noise factor of the amplifier. Reducing this value to the beginning of the span, we obtain $h\nu BAF$, where A is the attenuation coefficient in the span. For brevity, we will use $C \equiv h\nu BAF$. Then,

$$\frac{1}{\mathrm{OSNR}_{\mathrm{L}}} = \frac{C}{P}. \tag{3}$$

The value of $\mathrm{OSNR}_{\mathrm{L}}$ can be measured experimentally by an optical spectrum analyser. In the back-to-back configuration, nonlinear distortions are absent and $\mathrm{OSNR}_{\mathrm{BER}} = \mathrm{OSNR}_{\mathrm{L}}$, allowing one to measure the calibration curve. In a real link, $\mathrm{OSNR}_{\mathrm{BER}} < \mathrm{OSNR}_{\mathrm{L}}$ due to nonlinear distortions in accordance with (2). The difference between $\mathrm{osnr}_{\mathrm{L}}$ and $\mathrm{osnr}_{\mathrm{BER}}$ is called a penalty in power. Measuring $\mathrm{OSNR}_{\mathrm{L}}$ with a spectrum analyser and determining $\mathrm{OSNR}_{\mathrm{BER}}$ using a calibration curve at the BER level on the transponder, it is possible to calculate the value of nonlinear distortions.

The parameter $\mathrm{OSNR}_{\mathrm{NL}} = P/P_{\mathrm{NL}}$ is the ratio of the signal power to the nonlinear noise power. The value of nonlinear noise in the GN-model depends on the signal power P by the phenomenological law $P_{\mathrm{NL}} = \eta P^3$, where η is the nonlinearity coefficient. Thus, we obtain

$$\frac{1}{\mathrm{OSNR}_{\mathrm{NL}}} = \eta P^2. \tag{4}$$

The condition of the link performance is expressed by the inequality

$$\mathrm{OSNR}_{\mathrm{BER}} > \mathrm{OSNR}_{\mathrm{BTB}}. \tag{5}$$

Using (2), condition (5) can be written as

$$\frac{1}{\mathrm{OSNR}_{\mathrm{L}}} < \frac{1}{\mathrm{OSNR}_{\mathrm{BTB}}} - \frac{1}{\mathrm{OSNR}_{\mathrm{NL}}}. \tag{6}$$

*In this case, the output and input of the transponder are connected with a short connection cable, and nonlinear distortions of the signal are absent.

To denote the quantity in the right-hand side of formula (6), we use the concept of 'the required OSNR', defined as

$$\frac{1}{\mathrm{OSNR_R}} \equiv \frac{1}{\mathrm{OSNR_{BTB}}} - \frac{1}{\mathrm{OSNR_{NL}}}. \tag{7}$$

In view of (7), the condition of the link performance (6) can be written as

$$\mathrm{OSNR_L} > \mathrm{OSNR_R}. \tag{8}$$

In other words, $\mathrm{OSNR_R}$ is the minimum value of $\mathrm{OSNR_L}$ in a link which is still workable. In the back-to-back configuration, we have $\mathrm{OSNR_R} = \mathrm{OSNR_{BTB}}$. In a real line, $\mathrm{OSNR_R} > \mathrm{OSNR_{BTB}}$ due to nonlinear distortions of the signal. The dependence of $\mathrm{osnr_R}$ on the input signal power P is shown in Fig. 2a. The difference between $\mathrm{osnr_R}$ and $\mathrm{osnr_{BTB}}$ is called a penalty in the required OSNR for a given link (nonlinear penalty, NP).

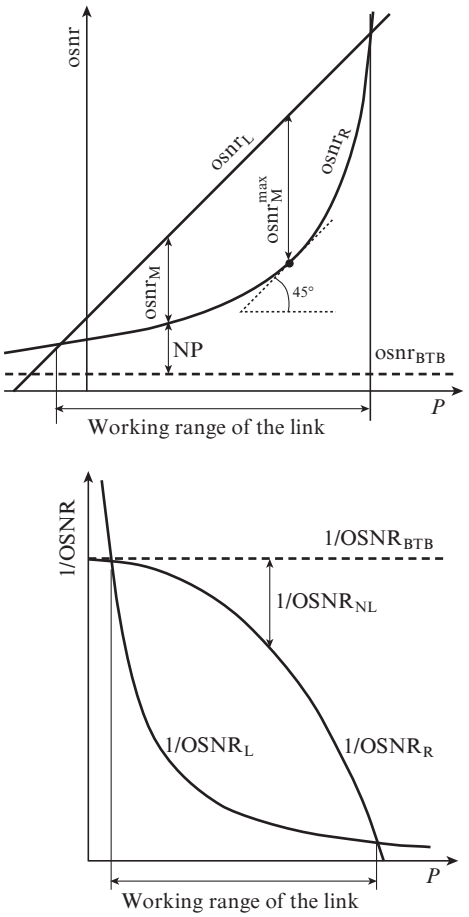

Figure 2. Basic quantities used to describe a communication link with allowance for the nonlinear distortion of the signal.

The value $1/\mathrm{OSNR_R}$ can be conveniently used as a link parameter characterising the quality of the optical signal. Before the advent of coherent systems, a measure of the signal quality was usually the bit error rate (BER) or Q-factor related to each other with one-to-one correspondence. However, the Q-factor in the linear regime is directly proportional to the signal power, which masks the influence of nonlinear effects with increasing power. The $\mathrm{OSNR_R}$ parameter in the linear regime does not depend on the signal power, and therefore its change shows the influence of the nonlinear effects in pure form. Due to this, it is more convenient to use this parameter, than BER and Q-factor, for studying the influence of nonlinear effects: it more accurately describes the signal quality that is not masked against the background of the varying signal-to-noise ratio. The smaller the $\mathrm{OSNR_R}$, the higher the quality of the optical signal. In this case, the Q-factor can be treated as a parameter that characterises the information quality of the signal.

In designing the links, use is also made of the concept of 'OSNR margin':

$$\mathrm{OSNR_M} \equiv \frac{\mathrm{OSNR_L}}{\mathrm{OSNR_R}}. \tag{9}$$

Using $\mathrm{OSNR_M}$, the link performance criterion (8) can be written in the simple form: $\mathrm{OSNR_M} > 1$, or $\mathrm{osnr_M} > 0$.

All the above quantities are presented in Fig. 2. The logarithmic values are more convenient to use in order to demonstrate the value of $\mathrm{osnr_M}$, and the absolute values – to demonstrate the value of $1/\mathrm{OSNR_{NL}}$. If we plot P^2 rather than P along the horizontal axis in Fig. 2b, the dependence of $1/\mathrm{OSNR_N}$ on P^2 will look like a straight line*, the slope of which is equal to the nonlinearity coefficient η.

The dependences of $\mathrm{OSNR_{BER}}$ and $\mathrm{OSNR_M}$ on the signal power P have maxima that are achieved at different values of P. Therefore, known are two main ways to link optimisation (calculation of optimal signal powers at the input in each span): based on the criterion of $\mathrm{OSNR_{BER}}$ maximisation (and therefore BER minimisation) and on the criterion of $\mathrm{OSNR_M}$ maximisation (OSNR margin). The second method allows one to design more robust links, but requires greater powers to be launched into spans.

Substituting (3) and (4) into (2), we obtain

$$\frac{1}{\mathrm{OSNR_{BER}}} = \frac{C}{P} + \eta P^2. \tag{10}$$

It is easy to calculate that the $\mathrm{OSNR_{BER}}$ maximum is achieved at a power

$$P_{\mathrm{BER}}^{\mathrm{opt}} = \sqrt[3]{\frac{C}{2\eta}}. \tag{11}$$

At the optimum point in BER, the linear noise power C is twice the nonlinear noise power ηP^3 and the penalty in power $(\mathrm{osnr_L} - \mathrm{osnr_{BER}})$ equals 1.76 dB. Substituting (3), (7) and (4) into (9), we obtain

$$\mathrm{OSNR_M} = \frac{C}{P}\left(\frac{1}{\mathrm{OSNR_{BTR}}} - \eta P^2\right). \tag{12}$$

It is easy to calculate that the $\mathrm{OSNR_M}$ maximum is achieved at a power

$$P_{\mathrm{M}}^{\mathrm{opt}} = \sqrt{\frac{1}{3\eta \mathrm{OSNR_{BTB}}}}. \tag{13}$$

At the optimum point in $\mathrm{OSNR_M}$, the penalty in the required OSNR $(\mathrm{osnr_R} - \mathrm{osnr_{BTB}})$ is 1.76 dB. There are also other opti-

* In systems with the developed nonlinear noise.

misation methods. Their advantages and disadvantages are considered in detail in paper [27].

3. Engineering approach to the design

To determine the operability of the designed communication link, to calculate optimal signal powers by using different optimisation criteria and to find the corresponding OSNR margins, it is necessary to know the nonlinearity coefficient η of the link. Theoretically, with a number of assumptions taken into account, it can be calculated based on fibre characteristics and parameters of the transmission system [16]. In reality, the existing links allow for some differences from theoretical assumptions. In calculations by theoretical formulas, the difference between theoretical and experimental results is so huge that these formulae are virtually inapplicable.

An engineering approach to the calculation of η consists in the fact that the dependence of η on various parameters (dispersion at the fibre input, span length and attenuation in fibre, number and location of adjacent channels, etc.) is studied experimentally. These experimental results make it possible to construct empirical formulas for this dependence for different transponders. Then, the obtained empirical formulas are used in the calculation of real links.

A key issue in the development of an engineering technique is the choice of a criterion for assessing its applicability. The calculated values are always different from the actual, and therefore it is needed to set tolerance criteria. As a criterion for assessing the applicability of the engineering technique we use the difference between the calculated and experimental values of $OSNR_R$ at the optimum point in $OSNR_M$ (13) (Fig. 3).

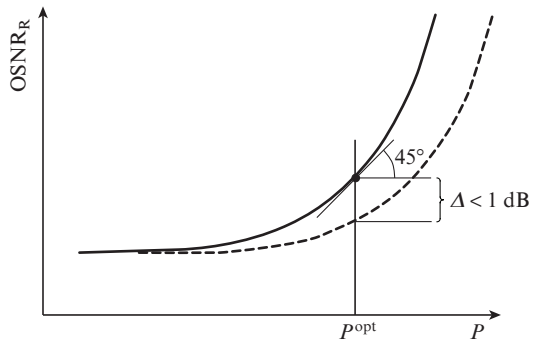

Figure 3. Evaluation criterion of applicability of the engineering calculation method. The solid curve is the theory, and the dashed curve is the experiment.

If the $OSNR_R$ value calculated by the empirical formulas of the engineering technique exceeds the experimental value by no more than 1 dB, the technique is considered to be practically applicable for this configuration of the DWDM system. If the calculated $OSNR_R$ exceeds the experimental value by more than 1 dB or is less, the method is treated as practically inapplicable for this configuration of the DWDM system. The main difficulty in the development of an engineering technique is that the applicability criterion should be fulfilled for all experimental configurations, the number of which can reach several hundred, and the value of the nonlinearity coefficient for them can vary by three orders of magnitude or more.

In reality, for a pilot link we measure directly η rather than $OSNR_R$ (see Section 4 below). The applicability criterion described above is satisfied if the ratio $\eta^{\text{theor}}/\eta^{\text{exp}} = 1-2$, which is readily obtained from formulae (7), (4) and (13).

The nonlinearity coefficient η for a 100-Gbit s^{-1} channel in each span depends on many independent parameters. The most important of them include:

– type of the optical unit in the transponder;
– size of the phase recovery window;
– type of fibre (SSMF, DCF, etc.);
– dispersion at the span input;
– span length;
– attenuation in fibre;
– number of 100-Gbit s^{-1} channels in the channel group in question; and
– frequency plan;

as well as (at the presence of other interacting channels):

– type of interacting channels (100, 10, and 2.5 Gbit s^{-1}, etc.);
– number of channels in the group;
– ratio of the power of interacting channels to the power of the 100-Gbit s^{-1} channel; and
– guard interval between the 100-Gbit s^{-1} channel under study and the group of interacting channels.

In a multi-span link, nonlinear noises in different spans are added superlinearly rather than linearly because they are correlated. This superlinear addition is performed differently for different types of interacting channels (100, 10 and 2.5 Gbit s^{-1}).

A detailed description of engineering calculation methods is beyond the scope of this paper. However as an illustration, we consider two examples: the dependence of η in the span on the dispersion at the span input and the calculation of η in a multi-span link with an arbitrary dispersion at the input to the spans.

The dependence of η in a single span on the dispersion at the span input was investigated numerically and experimentally in our work [8, 9]. We have shown that in a single-span link, the nonlinearity coefficient reaches the minimum value when the dispersion at the span input is $d \approx -180$ ps nm^{-1} (100 km SSMF, with a channel data rate of 100 Gbit s^{-1}). By increasing d to 2 ns nm and higher or decreasing to -2 ps nm^{-1} and below, the nonlinearity coefficient reaches a constant value and is further almost independent of a change in the dispersion at the span input (Fig. 4).

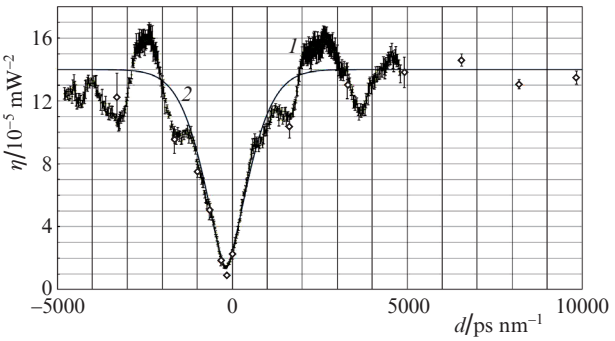

Figure 4. Dependences of the nonlinearity coefficient η in a single span on the dispersion d at the span input (100 km SSMF): (*1*) numerical simulation, (points) experiment and (*2*) approximation.

The dependence of η on d for a single span can be approximated by the expression

$$\eta(d) = \eta_0\left[1 - \exp\left(-\mu - \left|\frac{d - d_0}{\rho d_0}\right|^{3/2}\right)\right]. \quad (14)$$

Here, $\eta_0 = 14 \times 10^{-5}$ mW^{-2} is the fundamental nonlinearity coefficient corresponding to the nonlinearity coefficient of a channel in a span with a large dispersion at the span input; and $\mu = 0.1, \rho = 5$ and $d_0 = -180$ ps nm^{-1}. Formula (14) is used in the engineering method for calculating the nonlinearity coefficient in a span as a function of dispersion at the span input. The values of the fundamental coefficients for the different types of transponders and fibres are calculated experimentally.

In a multi-span link without dispersion compensation, the accumulation of nonlinear noise is not linear but superlinear ($\propto N^{1+\varepsilon}$, where N is the number of spans), as shown in recent studies [1, 2, 21]. In our engineering technique, for a 100-Gbit s^{-1} coherent link we assumed $\varepsilon \approx 0.2$.

In practice, there exist links with partial dispersion compensation, for example when a 100-Gbit s^{-1} channel is added to the existing DWDM system with 10-Gbit s^{-1} channels. Therefore, the development of the calculation technique allowing one to calculate η in a multi-span link with arbitrary values of dispersion at the input to various spans is important. Attempts to constructing such a technique have been made in recent paper [9]. Using OptSim software we have calculated multi-span links with a different number of spans where dispersion after each span is equally over- or undercompensated. The dependences of the nonlinearity coefficients for these links on additional dispersion in each span have a characteristic S shape. The simulation results for an eight-span link are shown in Fig. 5. This S-shaped dependence cannot be satisfactorily explained either by the model of linear addition of noises:

$$\frac{1}{\mathrm{OSNR_{NL}}} = \sum_i \frac{1}{\mathrm{OSNR_{NL}}i},$$

or by the model of superlinear addition of noises:

$$\frac{1}{\mathrm{OSNR_{NL}}} = \left[\sum_i \left(\frac{1}{\mathrm{OSNR_{NL}}i}\right)^{1/(1+\varepsilon)}\right]^{1+\varepsilon}.$$

For the superlinear model in Fig. 5 we use the coefficient $\varepsilon = 0.81$ calculated on the basis of experimental data for the links with total dispersion compensation. One can see that the model of superlinear addition is applicable only under conditions of total dispersion compensation or slight undercompensation (up to 100 ps nm^{-1}).

To correctly describe the accumulation of nonlinear noise in the links with a random distribution of accumulated dispersions at the inputs of various spans, we proposed a correlation model:

$$\frac{1}{\mathrm{OSNR_{NL}}} = \sum_i \frac{1}{\mathrm{OSNR_{NL}}i} + 2\sum_{j>i} \sigma_{ij} \sqrt{\frac{1}{\mathrm{OSNR_{NL}}i}\frac{1}{\mathrm{OSNR_{NL}}j}}. \quad (15)$$

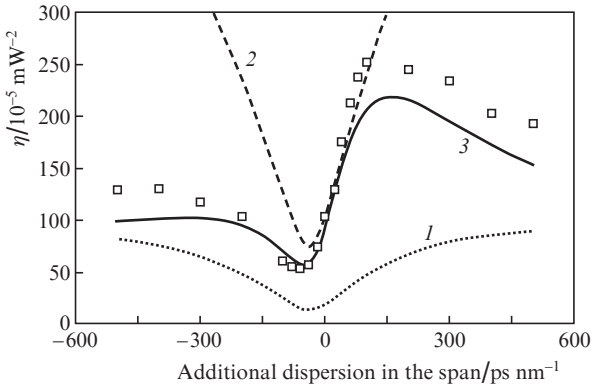

Figure 5. Dependences of the nonlinearity coefficient for an eight-span link on the additional dispersion in each span (a 100-Gbit s^{-1} channel): (points) numerical simulation, (*1*) linear, (*2*) superlinear and (*3*) correlation model.

If the input powers in all spans are equal, then formula (15) takes the form

$$\eta = \sum_i \eta_i + 2\sum_{i<j} \sigma_{ij} \sqrt{\eta_i \eta_j}, \quad (16)$$

where the coefficient σ_{ij} is the noise correlator from the ith and jth spans. Suppose that σ_{ij} depends only on the values of the accumulated dispersion $d_{i,j}$ at the input to the ith and jth spans ($i < j$) and is independent of the numbers i and j:

$$\sigma_{ij} = \sigma(d_i, d_j). \quad (17)$$

In this case, we can investigate numerically and experimentally the correlation function for a two-span link, and then use these results to calculate the nonlinearity coefficients in an arbitrary multi-span link with any number of spans. For example, for a two-span link we have $\eta = \eta_1 + \eta_2 + 2\sigma\sqrt{\eta_1\eta_2}$, for a three-span link $\eta = \eta_1 + \eta_2 + \eta_3 + 2\sigma\sqrt{\eta_1\eta_2} + 2\sigma\sqrt{\eta_1\eta_3} + 2\sigma\sqrt{\eta_2\eta_3}$ and so on. For a two-span link, σ can be calculated based on numerical simulation and experimental data from the formula:

$$\sigma = \frac{\eta - \eta_1 - \eta_2}{2\sqrt{\eta_1\eta_2}}. \quad (18)$$

A two-span link was numerically modelled using the OptSim software. The simulation results for σ as a function of d_1 and d_2 are shown in Fig. 6.

The correlation function obtained in the course of the simulation can be approximated by the formula

$$\sigma = a_1 \exp\left[-\left(\frac{d_1 - d_2 + a_2}{a_3}\right)^2\right], \quad (19)$$

where the coefficients $a_1 = 0.6$, $a_2 = 150$ ps nm^{-1} and $a_3 = 500$ ps nm^{-1}.

The three-dimensional surface of the correlation function, obtained as a result of numerical simulation, and its approximation by formula (19) is shown in Fig. 7. The developed correlation model [formulas (16) and (19)] can correctly describe the results of the simulation of multi-span links (Fig. 5). A detailed analysis of the correlation model and its experimental study are presented elsewhere [9].

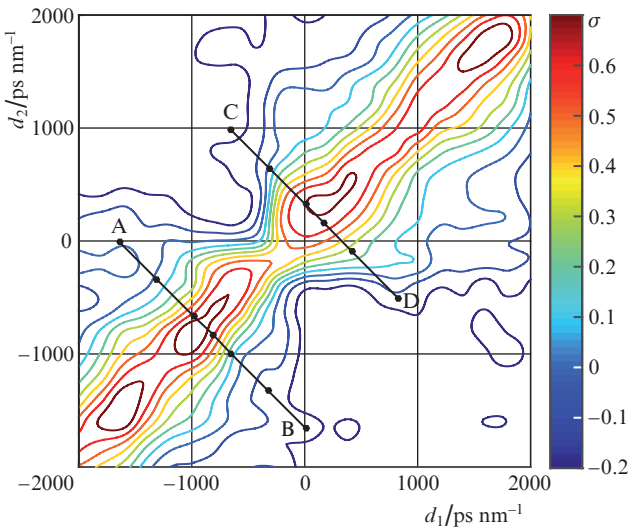

Figure 6. (Colour online) Numerical simulation of the correlation function (OptSim software); AB and CD are the experimentally measured cross sections [9].

4. Experimental measurement of the nonlinearity coefficient

The experimental setup for measuring the nonlinearity coefficient η is shown in Fig. 8. An optical spectrum analyser (OSA) is used to measure $OSNR_L$; the bit error rate before forward error correction (we call this value BER_{preFEC}) is measured by the transponder. Apart from a 100-Gbit s^{-1} channel, adjacent channels with data rates of 2.5, 10 and 100 Gbit s^{-1} may also be added. At the end of the link, use is made of a Teraxion tunable dispersion compensator module (TDCM) for adjusting dispersion at the transponder input to the optimal value ($\sim$700 ps nm^{-1}) and of an optical EDFA amplifier for adjusting the signal power at the transponder input to the optimal value known from previous experiments (–10 ÷ –15 dBm). A second demultiplexer (DEMUX) at the end of the link is used to 'cutoff' the broadband ASE noise and to reduce the total power at the input to the receiver to an acceptable level. To measure the calibration curve in the back-to-back scheme, a source of broadband ASE noise injects additional noise to the link via a variable optical attenuator (VOA).

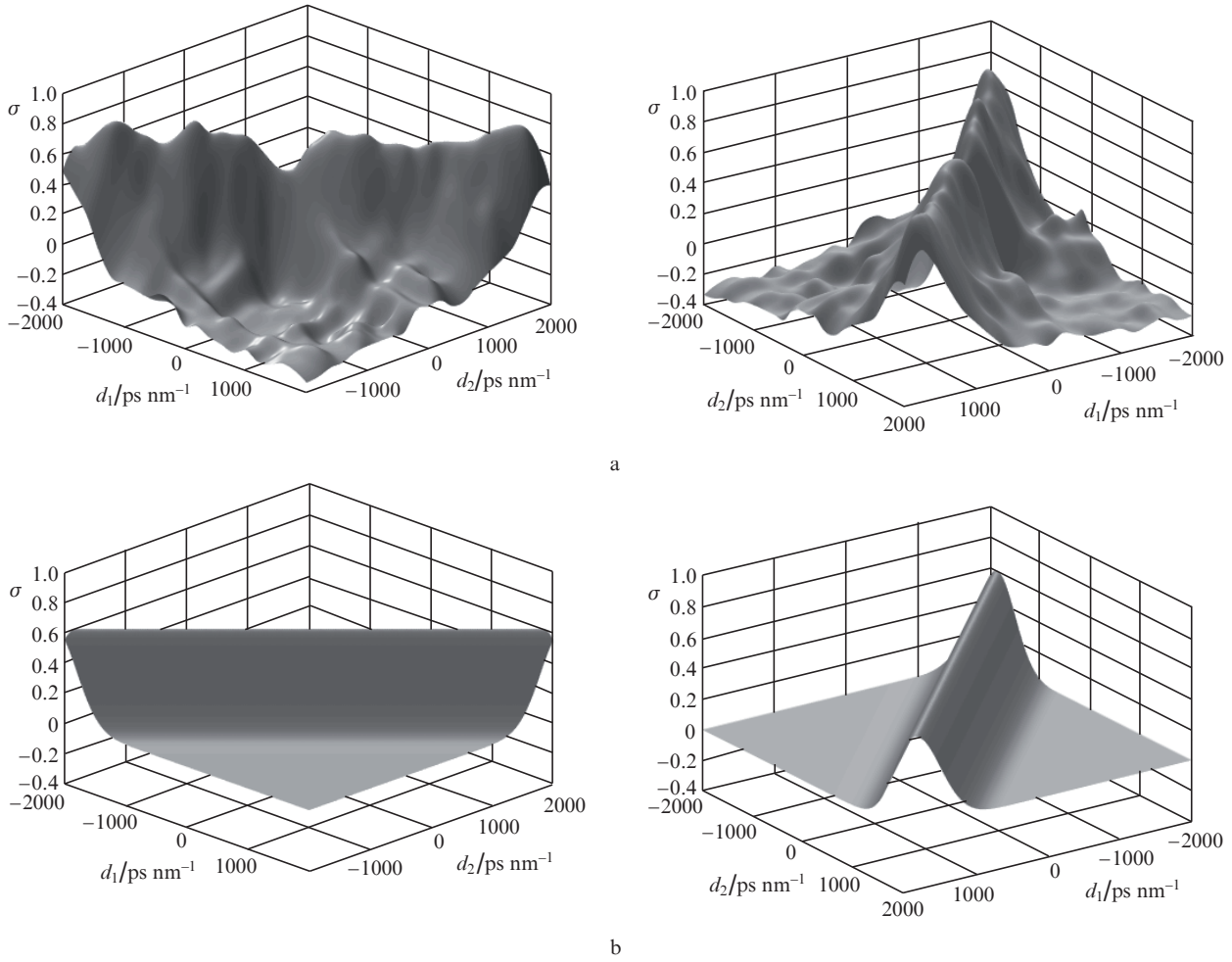

Figure 7. Three-dimensional surface of the correlation function at different angles: (a) OptSim simulation and (b) simple approximation of the correlation function.

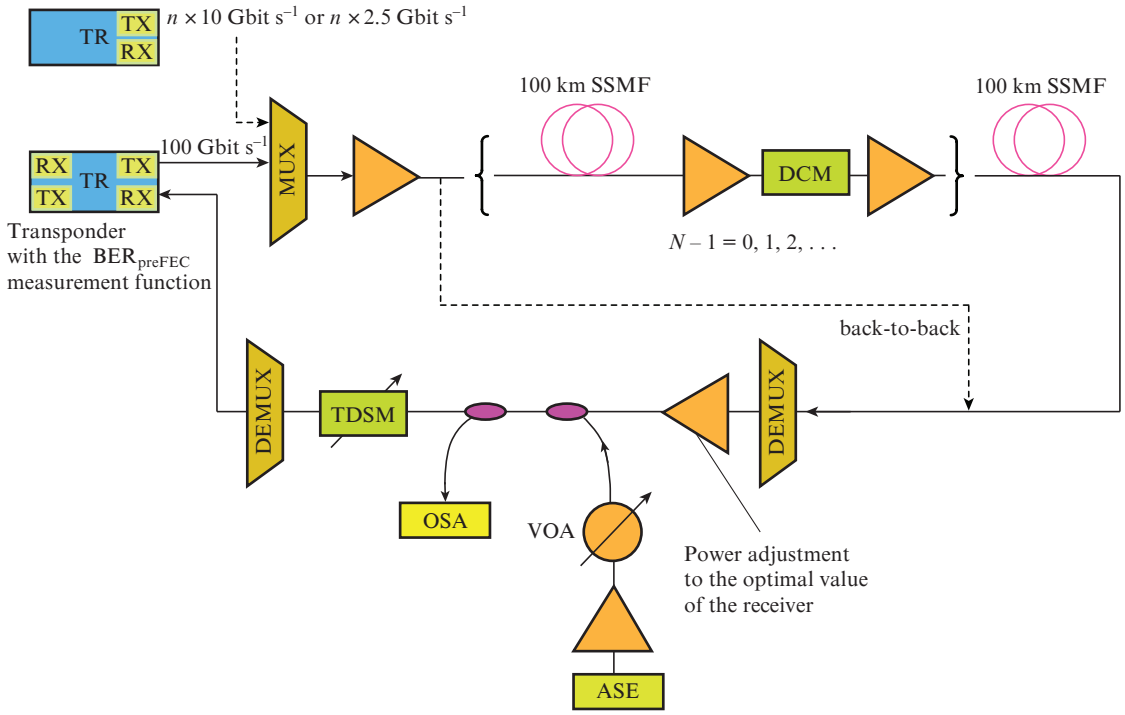

Figure 8. Scheme of the experimental setup (N is the number of spans and n is the number of channels).

The procedure for measuring the nonlinearity coefficient is as follows.

1. The dependence of $\mathrm{BER}_{\mathrm{preFEC}}$ on $\mathrm{OSNR}_{\mathrm{BER}}$ is measured in the back-to-back configuration. The obtained data are used to plot a calibration curve of the transponder: the dependence of $\mathrm{OSNR}_{\mathrm{BER}}$ (in dB) on $\lg\mathrm{BER}_{\mathrm{preFEC}}$. The experimental points are approximated by a polynomial of the third degree. For each transponder and each phase recovery window the calibration curve is individual.

2. The dependence of $\mathrm{OSNR}_{\mathrm{L}}$ at the transponder input on the power P is measured.

3. The transponder measures the dependence of $\mathrm{BER}_{\mathrm{preFEC}}$ on the input power P. The working range of $\mathrm{BER}_{\mathrm{preFEC}}$ lies between $10^{-5}-10^{-3}$; thus, the range of variation in the input power is selected so that the $\mathrm{BER}_{\mathrm{preFEC}}$ values were in the working range.

4. The calibration curve is used to recalculate the $\mathrm{BER}_{\mathrm{preFEC}}$ values into $\mathrm{OSNR}_{\mathrm{BER}}$ values.

5. The dependence of $\mathrm{OSNR}_{\mathrm{L}}$ on P (see Section 2) is used to calculate $\mathrm{OSNR}_{\mathrm{NL}}$ from the values of $\mathrm{OSNR}_{\mathrm{BER}}$ by formula (2).

6. The dependence of $1/\mathrm{OSNR}_{\mathrm{NL}}$ on P^2 is plotted. The points are approximated by a straight line whose slope represents the nonlinearity coefficient η.

The example of calculating the nonlinearity coefficient from the experimental data for a five-span link with the developed nonlinear noise is shown in Fig. 9.

A typical complication in the interpretation of experimental results is that nonlinear noise in the first few spans has not yet been formed, and the very concept of η is conditional. An example of calculating the nonlinearity coefficient from the experimental data for a single-span link with the underdeveloped nonlinear noise is shown in Fig. 10. The nonlinearity coefficient (the slope of the fitting line) is obtained by the linear approximation method of least squares, provided the straight line passes through the origin of the coordinates.

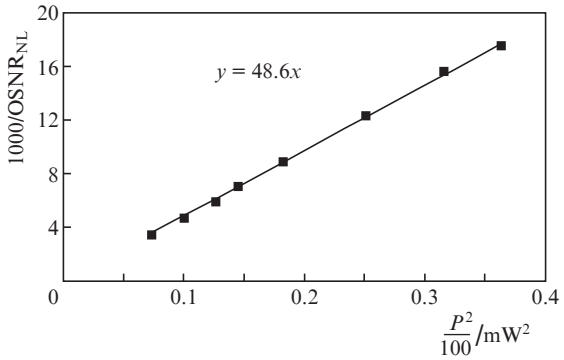

Figure 9. Calculation of the nonlinearity coefficient (Acacia CFP transponder, phase recovery window $W = 48$, five spans of 100 km SSMF, one 100-Gbit s^{-1} channel); $\eta = 48.6 \times 10^{-5}\ \mathrm{mW}^{-2}$.

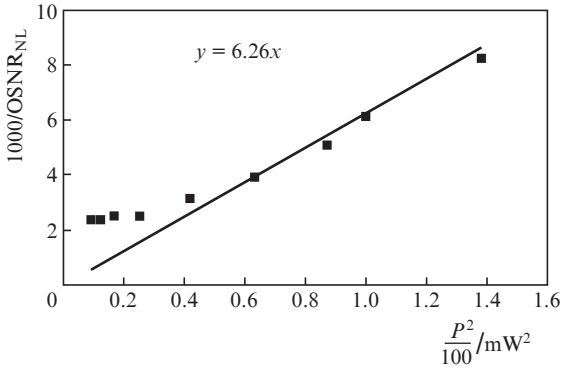

Figure 10. Calculation of the nonlinearity coefficient (Acacia CFP transponder, phase recovery window $W = 12$, one span of 100 km SSMF, one 100-Gbit s^{-1} channel and five 10-Gbit s^{-1} channels with a guard interval of 200 GHz); $\eta = 6.26 \times 10^{-5}\ \mathrm{mW}^{-2}$.

One can see from Fig. 9 that for a multi-span link, the GN-model describes with good accuracy the experimental results: nonlinearity, measured experimentally, can be treated as noise, and $1/\mathrm{OSNR}_{\mathrm{NL}} = \eta P^2$. From Figure 10 it is clear that for a single-span link, the GN-model does not quite accurately describe the experimental results and can be used only with reservations: nonlinearity, measured experimentally, deviates from the theoretical law $1/\mathrm{OSNR}_{\mathrm{NL}} = \eta P^2$. This is not surprising, because the GN-model was originally developed in the approximation of a large number of channels with the Nyquist (rectangular) shape of the spectrum in a multi-span link.

5. Conclusions

As noted above, the verification of the engineering calculation method consists in its application for calculating experimental configurations of communication lines and in comparing the calculated values with those measured experimentally. For convenience of verification and refinement of the method, all experimental configurations and measured nonlinear coefficients are collected in a single database (Excel file), and the calculation method is implemented in MATLAB. By executing a MATLAB script, we calculate the values of nonlinearity coefficients for all configurations specified in the Excel file, which are written back to the file in a separate column. In this way, we have assessed the applicability of the method: all measured values are compared with the calculated ones and the deviations range is automatically calculated.

Currently our database has more than one hundred experimental configurations. The measured values of the nonlinearity coefficient lie in the range from 0.8×10^{-5} to 933.82×10^{-5} mW^{-2}. Deviations from the estimated $\mathrm{OSNR}_{\mathrm{R}}$ values measured for all experimental configurations are within the specified range (Fig. 3): they amount to 0.12–0.76 dB. Thus, we can conclude that the proposed engineering method of calculation can be successfully applied in practice.

References

1. Gurkin N.V., Kapin Yu.A., Nanii O.E., Novikov A.G., Pavlov V.N., Plaksin S.O., Plotskii A.Yu., Treshchikov V.N. *Kvantovaya Elektron*., **43**, 546 (2013) [*Quantum Electron*., **43**, 546 (2013)].
2. Pilipetskii A. *Proc. Optical Fiber Communications Conf. (OFC'15)* (Los Angeles, Cal., USA, 2015) paper W3G.5.
3. Gainov V.V., Gurkin N.V., Lukinih S.N., Makovejs S., Akopov S.G., Ten S.Y., Nanii O.E., Treshchikov V.N., Sleptsov M.A. *Opt. Express*, **22**, 22308 (2014).
4. Gainov V.V., Gurkin N.V., Lukinih S.N., Akopov S.G., Makovejs S., Ten S.Y., Nanii O.E., Treshchikov V.N. *Laser Phys. Lett*.. **10**, 075107 (2013).
5. Reis J.D. (Ed.) *400G White Paper. Technology Options for 400G Implementation (OIF-Tech-Options-400G-01.0)* (Fremont, Cal., USA, 2015).
6. Bayvel P., Behrens C., Millar D.S., in *Optical Fiber Telecommunications VI B: Systems and Networks* (New York: Acad. Press, 2013) pp 221–288.
7. Vacondio F., Rival O., Simonneau C., Grellier E., Bononi A., Lorcy L., Antona J.-C., Bigo S. *Opt. Express*, **20** (2), 1022 (2012).
8. Konyshev V.A., Leonov A.V., Nanii O.E., Novikov A.G., Treshchikov V.N., Ubaydullaev R.R. *Opt. Commun*., **349**, 19 (2015).
9. Konyshev V.A., Leonov A.V., Nanii O.E., Novikov A.G., Treshchikov V.N., Ubaydullaev R.R. *Opt. Commun*., **381**, 352 (2016).
10. Antona J.-C. et al. *Proc. Optical Fiber Communications Conf. (OFC'02)* (Anaheim, Cal., USA, 2002) paper WX5.
11. Antona J.-C. et al. *Proc. ECOC'06* (Cannes, France, 2006) We.3, p. 41.
12. Antona J.-C. et al. *Proc. Optical Fiber Communications Conf. (OFC'08)* (San Diego, Cal., USA, 2008) paper JThA48.
13. Antona J.-C., Bigo S. *Comptes Rendus Physique*, **9**, 963 (2008).
14. Redyuk A.A., Nanii O.E., Treshchikov V.N., Mikhailov V., Fedoruk M.P. *Laser Phys. Lett*., **12**, 025101 (2015).
15. Yushko O.V., Nanii O.E., Redyuk A.A., Treshchikov V.N., Fedoruk M.P. *Kvantovaya Elektron*., **45** (1), 75 (2015) [*Quantum Electron*., **45** (1), 75 (2015)]..
16. Poggiolini P., Bosco G., Carena A., Curri V., Jiang Y., Forghieri F. *J. Lightwave Technol*., **32**, 694 (2014).
17. Splett A., Kurzke C., Petermann K. *Proc. ECOC* (Montreaux, Switzerland, 1993) Vol. 2, pp 41–44.
18. Poggiolini P., Carena A., Curri V., Bosco G., Forghieri F. *IEEE Photonics Technol. Lett*., **23**, 742 (2011).
19. Carena A., Curri V., Bosco G., Poggiolini P., Forghieri F. *J. Lightwave Technol*., **30** (10), 1524 (2012).
20. Poggiolini P. *J. Lightwave Technol*., **30** (24), 3857 (2012).
21. Gurkin N.V., Nanii O.E., Novikov A.G., Plaksin S.O., Treshchikov V.N., Ubaydullaev R.R. *Kvantovaya Elektron*., **43** (6), 550 (2013) [*Quantum Electron*., **43** (6), 550 (2013)].
22. Konyshev V.A., Leonov A.V., Nanii O.E., Novikov A.G., Treshchikov V.N., Ubaydullaev R.R. *Opt. Commun*., **349**, 19 (2015).
23. Gurkin N.V., Konyshev V.A., Nanii O.E., Novikov A.G., Treshchikov V.N., Ubaydullaev R.R. *Kvantovaya Elektron*., **45** (1), 69 (2015) [*Quantum Electron*., **45** (1), 69 (2015)].
24. Gurkin N.V., Mikhailov V., Nanii O.E., Novikov A.G., Treshchikov V.N., Ubaydullaev R.R. *Laser Phys. Lett*., **11**, 095103 (2014).
25. Nespola A., Huchard M., Bosco G., Carena A., Jiang Y., Poggiolini P., Forghieri F. *Proc. Optical Fiber Communications Conf. (OFC'15)* (Los Angeles, Cal., USA, 2015) paper Th4D.2.
26. Redyuk A.A., Nanii O.E., Treshchikov V.N., Mikhailov V., Fedoruk M.P. *Laser Phys. Lett*., **12**, 025101 (2015).
27. Konyshev V.A., Leonov A.V., Nanii O.E., Treshchikov V.N., Ubaydullaev R.R. *Opt. Commun*., **355**, 279 (2015).